SOME TYPICAL SHELL STABILITY PROBLEMS ENCOUNTERED IN THE DESIGN OF BALLISTIC MISSILES

by
A. Kaplan, E. J. Morgan and W. Zophres
Space Technology Laboratories, Inc.

INTRODUCTION AND SUMMARY

Investigations carried out at STL on three current problems involving instability of thin shells in applications to aerospace vehicles are discussed. The first concerns the experimental determination of the buckling behavior of longitudinally stiffened pressurized cylinders; the second, the analytic prediction and experimental confirmation of the buckling behavior of multi-layer cylinders and the third involves the behavior of cylinders under combined axial load and lateral pressure. In each case the background of the application is reviewed, followed by a short description of the work. It is indicated that the longitudinally stiffened cylinder shows considerable promise in taking maximum advantage of the strengthening effect of internal pressure, that the use of an external low modulus layer as an insulator can have a significant effect on the buckling capability of a shell, and that the assumption of a linear interaction for pressure and axial load is unnecessarily conservative.

STIFFENED PRESSURIZED CYLINDRICAL SHELLS

The two original ballistic missiles, Atlas and Titan, were engineered with quite different design philosophies. In the Atlas, the primary axial load carrying ability is due to a high internal pressure and the thin walls serve primarily to contain the pressure, although they do make a small but significant contribution to the strength of the structure. This type of design can be quite efficient if high pressures are required for other systems such as the pump, and if high strength materials are employed. Its major disadvantage is the requirement of continual pressurization or axial tension in the structure to prevent collapse.

The Titan criteria specified that the fully-loaded missile be capable of standing erect in a wind with zero internal pressure. To meet this condition, the initial design called for a conventional aluminum aircraft type structure with longitudinal stringers supported by circumferential rings. However, due to the high pressurization stresses and severe aerodynamic heating this design is subjected to very large

secondary stresses at the frame attachments. These were eliminated by supporting the frames with radially slotted fittings. The frames supported the longerons in the unpressurized condition by preventing inward motion, but exerted no restraint to the outward motion resulting from internal pressure and heating. In the pressurized condition the only support for the longerons was obtained from the elastic foundation provided by the stressed skin. The procedure used for design was to size the stringers for the unpressurized ground condition assuming the tank behaved as a conventional stiffened structure, and then to check for the pressurized flight condition assuming that the skins buckled and that the elastically supported stringers failed by crippling. This structural concept was proved out by full scale room temperature tests and programmed heating tests conducted by the Martin Company at their own plant and at Wright field. It has been successfully used on both the Titan I and Titan II missiles. However, for the Titan tanks the unpressurized ground condition is critical, therefore there was no need to determine the effect of the various parameters of the pressurized stiffened structure and thus optimize its design.

To determine the full potentialities of this type of structure, a small scale testing program was started at STL a year and a half ago. It was felt that in addition to the reasons for its use in the Titan design, pressurized stiffened cylinders had the potential of making better use of the stiffening effect of the internal pressure than did the monocoque type of structure. This expectation was based on the observed buckling behavior of pressurized monocoque cylinders. With increasing internal pressure, the monocoque buckling waves become shorter longitudinally and larger circumferentially. When they approach an axially symmetric shape, the buckling stress which has been increasing with the pressure reaches a limit equal to the classical buckling stress for a monocoque cylinder. The addition of longitudinal stiffening would be expected to inhibit the formation of these axially symmetric buckles and thus increase the buckling stress of the skin. Furthermore, after buckling, the skin would be expected to act as a stretched membrane in the circumferential direction and thus continue to provide an elastic foundation for the longerons. These expectations were reinforced by the theoretical results of Thieleman (Reference 1) which indicated that internal pressure has a much stronger effect on the buckling stress of an orthotropic cylinder with the major stiffness in the longitudinal direction than on an isotropic cylinder.

a. Specimen Description

The aim of the test program was to determine the buckling behavior of longitudinally stiffened cylinders as a function of the internal pressure and the geometrical parameters of the cylinder. The latter included the R/t and L/R of the cylinder skin, and the number, size and

shape of the stiffeners. Because of the large number of combinations, it was necessary that a simple, easily made specimen be used. The test specimen and testing technique used were similar to that developed in a previous program and described in detail in Reference 2. The cylinders were formed from thin (2 mil to 10 mil) Mylar plastic and were bonded to plexiglas stringers. The specimens were joined to the end caps by casting them in a ring of Cerrelow, a low melting temperature metal alloy, thus providing a uniform loading of both stringers and skin.

The principal advantage in the use of Mylar is that due to its large range of linear elongation, buckling tests can be repeated without any degradation in performance. This had been demonstrated in the previous program and, in addition, it had been shown that there was no significant difference between the results for Mylar and those for metal, provided the buckling stresses were within the elastic limit.

The basic test cylinder was 8 inches in diameter and 8 inches long, but the effects of length and diameter were checked by spot testing of other sizes covering a range of R/t from 400 to 4,000 and of L/R from 1 to 4. Most of the stringers were of rectangular section, but a few tests using I and H sections were also made. The number of stringers was varied from 4 to 72.

b. Test Procedure

Tests on each specimen were made at a sequence of increasing pressures. The specimen was loaded at a constant displacement rate until the peak load was achieved. The total axial load and the relative axial displacement of the cylinder ends were continuously measured and recorded on an XY plotter. The results of a test sequence for a typical specimen with intermediate size stiffening are shown in Figure 1. The interruption in the curve indicates visual observance of panel buckling, while the horizontal intercept indicates the load carried by the pressure, $\pi R^2 p$.

c. Description of Results

The buckling of the specimens fell into several regions depending primarily upon the internal pressure and the relative size and number of the stringers.

For relatively light stringers at low pressures the specimens behaved as orthotropic cylinders with buckling of the skin and stringers occurring simultaneously. As the pressure was increased, the stringers continued to carry load after buckling of the skin and finally failed as columns. Finally, at high pressure, general failure occurred in an axisymmetric mode (Figure 2) similar to the failure of a monocoque cylin-

der at high pressure. The onset of the axisymmetric mode was accelerated by an increase in the number of stringers.

For the heavier stringers, skin buckling occurs appreciably earlier than general failure. The skin buckles in the familiar diamond pattern with the longitudinal wave length decreasing with increasing pressure. At low pressure, the stringers buckle in their first or second longitudinal mode. With increasing pressure, the stringer buckling wave length decreases, but at a slower rate than that of the skin. Typical failure mode of a heavily stiffened cylinder at intermediate pressure is shown in Figure 3.

d. Analysis of Results

In line with the experimental evidence, two approaches were used in the theoretical analysis of the problem. In the first, the cylinder was treated as an orthotropic shell and a one term solution obtained for the corresponding Donnell type equation. In the second, the stringers were treated as individual columns supported by the skin acting as an elastic foundation. Neither of these approaches has been very satisfactory as yet but they have indicated the qualitative trends of the data.

In lieu of an analytic theory, an empirical equation indicating the influence of the various parameters was developed. The initial step in this direction was to separate the load carrying capability of the skin from that of the stringers. This was done by subtracting the sum of the load carried by pressure and the calculated buckling load of the monocoque skin from the total failure load, and dividing the result by the number of stringers. This gave P_N, the increase in load above that of pure monocoque cylinder due to each stringer.

Plotting P_N for various numbers of stringers as a function of pressure indicated that over most of the range of configurations tested P_N was independent of the number of stringers and was proportional to the square root of the pressure, except at very low pressures. Continued plotting and analysis led eventually to the following formula

$$P_N = \frac{4\pi^2 E_o I_o}{L^2} + \frac{1}{2}\sqrt{\left(\frac{E_o I_o}{\rho_o}\right)\left(\frac{E_s t^2}{12(1-\mu^2)R}\right)}\left\{1 + \sqrt{1 + 12(1-\mu^2)\frac{p}{E_s}\left(\frac{R}{t}\right)^2}\right\}$$

The formula agrees within an accuracy of about 10% with all the experimental results except those for a large number of stringers and high

pressures. For those cases, the formula overestimates the increase in P_N with pressure. The overestimation occurs earlier with relatively light stringers and is evidently associated with the onset of the axially symmetric buckling mode. Methods of including this effect in the formula are still being studied. In Figure 4 the results for similar cylinders with a wide variation in size and number of stringers are compared with the predictions of the formula. The good agreement over most of the range of parameters together with the drop off for the large number of stringers is evident.

The difficulties in obtaining an accurate analysis using the concept of an elastically supported column are evident by comparing the empirical buckling formula with the equation for the buckling of a clamped column on an elastic foundation

$$P_{cr} = 4\frac{\pi^2 E_o I_o}{L^2} + 2\sqrt{k E_o I_o}$$

This indicates that the effective elastic foundation is a function of ρ_o and thus evidently cannot be the simple Winkler type foundation which is usually assumed. The comparison also indicates that for large pressures the stiffness is independent of the skin thickness and thus the effective width of the skin is independent of pressure. This conclusion is confirmed by the load deflection curves.

Additional analyses are being performed in an attempt to determine the mechanism of this effect and additional tests are planned to further delineate the region of axially symmetric buckling. To determine if the axial compression results are applicable to bending, a small bending program has been started. Initial results from this program are encouraging and indicate that the bending behavior can be inferred from the axial test results.

LOW R/t MONOCOQUE CYLINDERS SUBJECTED TO COMBINED EXTERNAL PRESSURE AND AXIAL LOAD

The interstage structure of the Minuteman consists of ring stiffened monocoque cone frustums of small included angle and with an R/t of about 200. For the loads encountered by the Minuteman, this monocoque design provides a good combination of high bending stiffness, high heat sink capability to minimize aerodynamic heating, and relatively low weight. The critical loading conditions for the interstages occur at stage burnout due to a combination of axial compressive load and high temperature,

at maximum dynamic pressure due to a combination of axial compression, bending and a slight external pressure, and at silo launch, due to a combination of axial compression and high external pressure. To optimize the design for the launch condition, a small scale testing program was instituted at STL.

An earlier test program (Reference 2) covering a wide range of cones and cylinders had indicated that the interaction curve for buckling of cylinders under axial compression and external pressure was concave upwards, particularly for low values of R/t. However, there was not enough data to be conclusive and there was no data for R/t less than 400. Additional testing was therefore indicated. Because of the small included angles of the interstages, and because the previous results had indicated good correlation between low angle cones and cylinders, it was decided to simplify the testing by using cylinders. The specimens were similar to those described in the previous section, being made of Mylar plastic sheet joined to the end plates by casting in a Cerrelow ring.

Tests were run on a series of specimens with R/t = 156 and approximately 200, and with values of Z ranging from 26 to 739. The results are presented in Figure 5 as the ratios of the experimentally determined buckling pressures and loads to design values for lateral pressure alone and axial load alone, respectively. The reference buckling coefficients for lateral pressure are taken as 90% of the values suggested by Batdorf (Reference 3) while the reference axial buckling coefficients are those recommended in Reference 2, that is

$$C = 0.606 - 0.546 \left(1 - \exp - \frac{1}{16} \sqrt{\frac{R}{t}} \right)$$

It is seen that the interaction curve is strongly non-linear and also asymmetrical. A line drawn through the mean of the data would be definitely non-circular. However, due to the increased scatter for the high axial load conditions, a circular interaction curve is recommended for design. A report describing the details of the experimental work is in preparation.

It is clear that in this low range of R/t the assumption of a linear interaction curve between axial load and lateral pressure is unnecessarily conservative.

COMPOSITE CYLINDERS SUBJECTED TO AXIAL COMPRESSION AND EXTERNAL PRESSURE

The Guidance and Control Compartment of the Minuteman is subjected to similar loading conditions as are the interstages. However, due to its forward position, the load intensities are lower and the aerodynamic heating is higher. As the result of several design studies, it was decided to use an aluminum monocoque shell with one intermediate lateral pressure ring to which was bonded a layer of low conductivity fiberglass insulation. An important factor in the choice of this configuration was the major contribution of the fiberglass insulation to the buckling strength of the shell for silo launch and max q conditions. At these times, particularly the silo launch condition, only the surface layers of the fiberglass were heated and therefore it maintained most of its room temperature properties. At the final burnout condition, the fiberglass was heated throughout and its structural contribution was therefore neglected.

The analytic approach (Reference 4) to the buckling of the two layered cylinder was based on neglecting the difference in Poisson's ratio between the two materials. This approximation allows a simple calculation of the bending and stretching stiffnesses of the composite shell. On substituting these stiffnesses into Donnell's equations, revised expressions were obtained for the curvature parameter Z and the buckling coefficient K. These revised expressions then allow direct utilization of the solutions obtained by Batdorf (Reference 3) and others for the buckling of thin cylindrical shells for various loading conditions.

Thus for a shell consisting of two thicknesses, t_1 and t_2 with elastic moduli E_1 and E_2, respectively, the composite extensional stiffness B is given by

$$B = \frac{E_1 t_1}{1-\mu^2}\alpha \, , \quad \alpha = 1 + \frac{E_2 t_2}{E_1 t_1}$$

while the composite bending stiffness D is given by

$$D = \frac{E_1 t_1^3}{12(1-\mu^2)}\beta \, , \quad \beta = 4 + 4\,\frac{E_2}{E_1}\left(\frac{t_2}{t_1}\right)^3 - \frac{3\left[1 - \frac{E_2}{E_1}\left(\frac{t_2}{t_1}\right)^2\right]^2}{1 + \frac{E_2 t_2}{E_1 t_1}}$$

Then

$$Z = \frac{L}{R}\sqrt{\frac{1-\mu^2}{12}}\sqrt{\frac{B}{D}} = \sqrt{1-\mu^2}\;\frac{L^2}{R\,t_1\sqrt{\frac{\beta}{\alpha}}}$$

and

$$N_{cr} = K\,\frac{\pi^2 D}{L^2} = K\,\frac{\pi^2 E_1 t_1^3}{12(1-\mu^2)L^2}\,\beta$$

For large Z, the equation for buckling under an axial load is simply

$$K_x = \frac{4\sqrt{3}}{\pi}\,Z$$

which, on making the proper substitutions becomes

$$N_{cr} = \frac{1}{\sqrt{3(1-\mu^2)}}\;\frac{E_1 t_1^2}{R}\sqrt{\alpha\beta} = 0.6\;\frac{E\,t_1^2}{R}\sqrt{\alpha\beta}$$

Thus, the theoretical influence of the second layer is proportional to $\sqrt{\alpha\,\beta}$. Presumably there is a similar reduction in the theoretical coefficient, 0.6, for the multilayer cylinder as there is for the homogeneous cylinder. The actual functional variation can only be determined experimentally, but a likely candidate is to assume the same function of R/t as for a single cylinder based on the effective thickness term in the expression for Z, $t_{eff} = t_1\sqrt{\beta/\alpha}$.

In Figure 6(a) are shown the results of axial buckling tests of full-scale cylinders representing the Minuteman G&C Compartment. The results are expressed as the ratio of the actual buckling loads to the average buckling load obtained for three single layer aluminum cylinders. The R/t of the aluminum cylinder is 244 and the L/R is 1.8. These tests were conducted by the Space and Information Division of North American Aviation. Also shown are the theoretical predictions for the two assumptions that the buckling coefficient is considered a function of $\sqrt{\alpha/\beta}$ and that it is considered independent of $\sqrt{\alpha/\beta}$. The data is insufficient to confirm the theoretical predictions over a range of thickness ratios, but it does confirm the major increase in load at the tested thickness ratio.

For the buckling of cylinders under lateral pressure, the Batdorf expression for the buckling coefficient for large Z is

$$K_y = 1.04\sqrt{Z}$$

On substitution, the expression for the lateral buckling pressure, p_{cr}, is obtained

$$p_{cr} = 0.926 \quad E_1\left(\frac{t_1}{R}\right)^{5/2} \quad \frac{R}{L} \quad \sqrt[4]{\beta^3\alpha}$$

Thus, for lateral pressure, the influence of the second layer is proportional to

$$\sqrt[4]{\beta^3\alpha} = \sqrt{\alpha\beta} \quad \sqrt[4]{\beta/\alpha}$$

and is considerably greater than for the axial load case.

In figure 6(b) are shown the results of similar tests performed by North American for the lateral pressure case. The results are presented in the same way as for the axial load case except that the reference value for a single layer is computed. Two of the specimens were cylinders ($R/t_1 = 240$, $L/R = 1.8$) and the other two were conical frustums with a semi angle of 5° ($R/t_1 \approx 240$, $L/R \approx 0.9$). In this case the tests were conducted at a variety of thickness ratios and indicate excellent agreement with the theoretical predictions.

It thus appears that the simple theory presented here gives good correlation with experiment and further that the addition of a relatively thick but low modulus layer has a significant effect on the buckling load of a cylinder, particularly under lateral pressure. It should be noted that for Minuteman interstages, the proportionate amount of insulation required is much smaller and therefore the use of fiberglass would have a much less significant effect on the buckling strength.

One severe problem should be mentioned before closing. The buckling capability of a two layer structure is a critical function of the bond between the layers. This is particularly the case when plastics are bonded to metals because the wide difference in thermal coefficients of expansion can induce significant internal stresses. It is only when these factors are considered in detail in laying out the fabrication and quality control procedures, as was done by North American, that a successful structure can be built.

REFERENCES

1. W. F. Thielemann, "New Developments in the Non-Linear Theories of the Buckling of Thin Cylindrical Shells," Aeronautics and Astronautics Proceedings of the Durant Centennial Conference, N. J. Hoff and W. G. Vincenti, Editors. Pergamon Press, New York, 1960

2. V. I. Weingarten, E. J. Morgan and P. Seide, "Final Report on Development of Design Criteria for Elastic Stability of Thin Shell Structures," Space Technology Laboratories, Inc. Report, TR-60-0000-19425, December 1960.

3. S. B. Batdorf, "A Simplified Method of Elastic-Stability Analysis for Thin Cylindrical Shells," NACA TR 874, 1947.

4. W. Zophres, "Elastic Buckling of Two-Layer Cylinders and Curved Plates," Space Technology Laboratories, Inc. Report, GM-TR-0165-00539, December 1958.

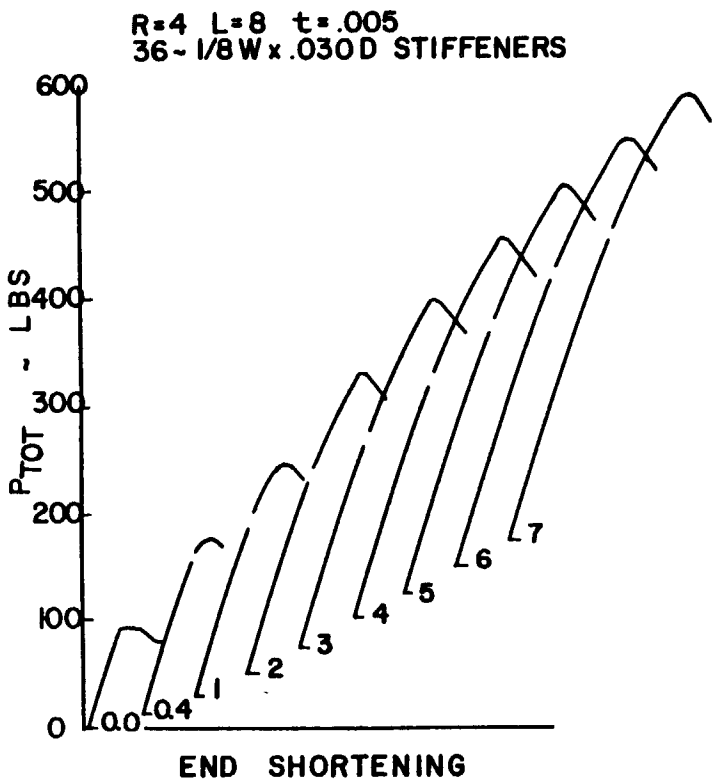

Figure 1.- Typical sequence of load-deflection curves.

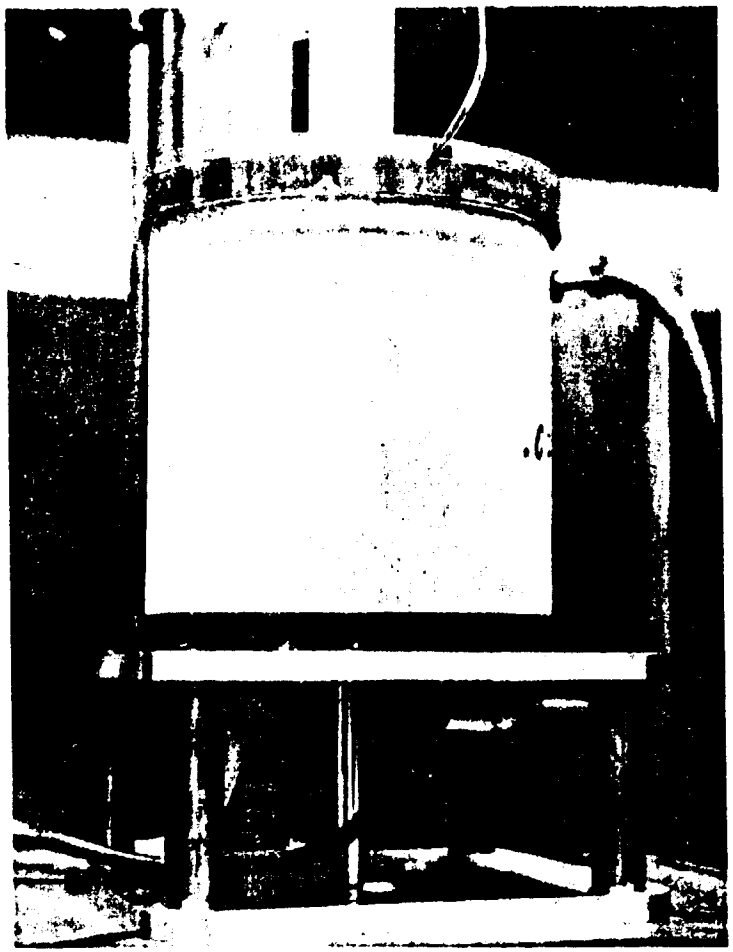

Figure 2.- Axisymmetric buckling mode of a lightly stiffened cylinder (same specimen as fig. 1).

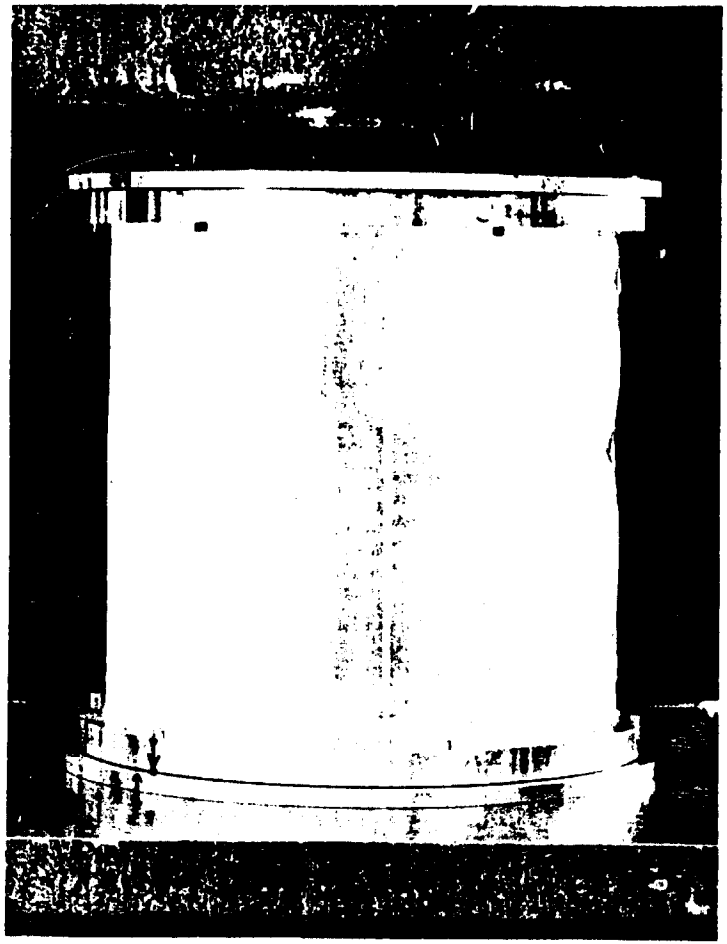

Figure 3.- Typical buckling mode of a heavily stiffened cylinder at intermediate pressure (specimen X of fig. 4).

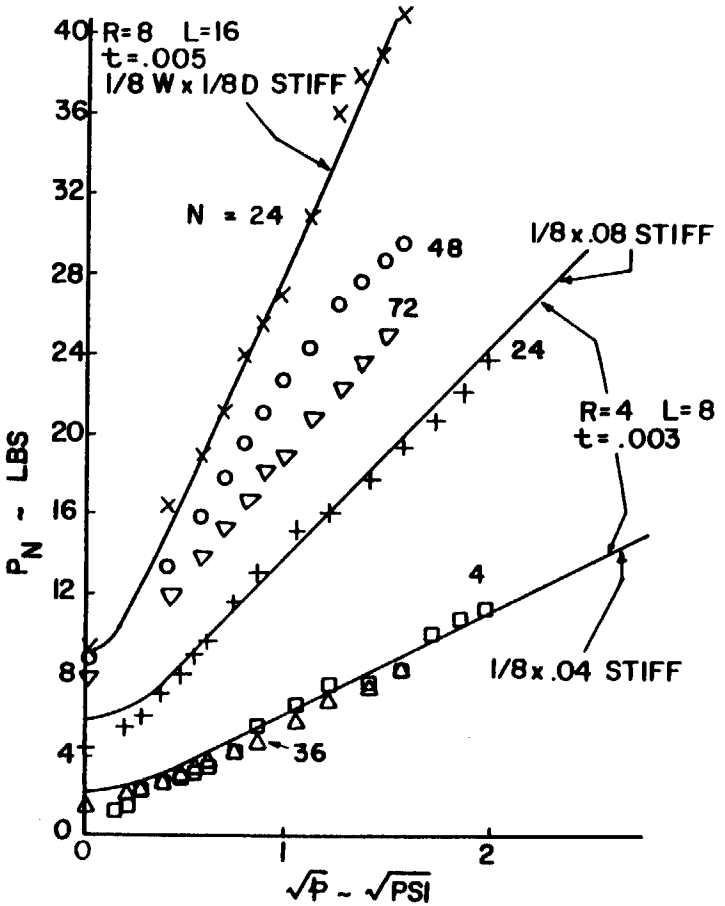

Figure 4.- Comparison of experimental results with empirical prediction.

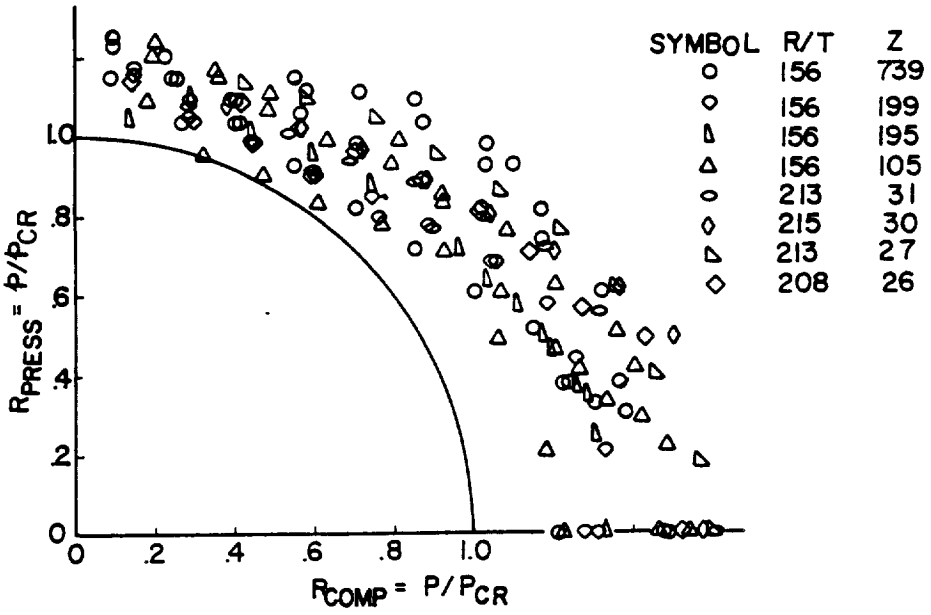

Figure 5.- Experimental results for Mylar cylinders under combined axial compression and external pressure.

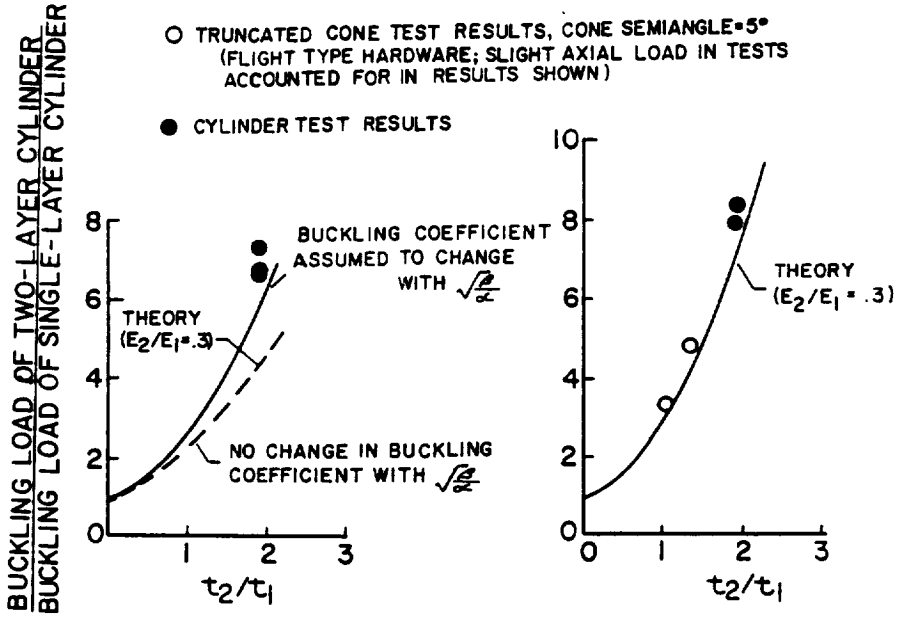

(a) Axial compression. (b) External pressure.

Figure 6.- Buckling of two-layer cylinders (cylinders of aluminum-reinforced plastic combination).